Adaptive Rejection of Disturbances Having Two Sinusoidal Components with Close and Unknown Frequencies[*]

Xiuyan Guo[†]and Marc Bodson[‡]

July 26, 2010

Abstract

The paper considers the problem of rejecting disturbances with two sinusoidal components in the case where the frequencies are unknown and closely spaced. A natural approach consists in cancelling the components using two separate adaptive algorithms combined in a single scheme. However, experiments in active noise control applications have shown that convergence using such an approach could be very slow. The alternative approach of this paper consists in representing the disturbance signal as a single sinusoid with time-varying magnitude and phase. The theoretical basis and the limitations of such a representation are first discussed. Then, an adaptive disturbance rejection algorithm is proposed and the resulting nonlinear system is analyzed using some approximations. Active noise control experiments demonstrate that the proposed algorithm has better convergence properties than an algorithm designed to cancel the two frequency components separately. In some cases, however, the cost is a small residual error on the output signal.

Keywords: active noise control, adaptive control, frequency estimation, magnitude phase-locked loop, periodic disturbance rejection.

1   Introduction

Periodic disturbances are encountered in many applications. In this paper, we focus on *active noise control* (ANC), which is a method for eliminating or attenuating noise by the destructive interference of controlled 'secondary' sources with the disturbance from the 'primary' source [4]. ANC is especially effective against low-frequency noise (below 500 Hz), which is hard to reduce by passive methods [7]. When a so-called reference signal is available, *feedforward control* methods

---

[†]X. Guo is with EnOcean Inc., 6914 S 3000 E Suite 202C, Cottonwood Height, UT 84121, USA.

[‡]M. Bodson (corresponding author) is with the Department of Electrical and Computer Engineering, University of Utah, 50 S Central Campus Dr Rm 3280, Salt Lake City, UT 84112, USA (email: bodson@ece.utah.edu).

are widely used and can attenuate broadband noise as well as narrowband noise [6]. However, this approach requires that the reference signal be well correlated with the primary source and, in some situations, it is difficult or undesirable to obtain such a reference signal. Then, *feedback control* is necessary, which means that the error signal must be used alone to attenuate the noise.

While *feedback control* of periodic disturbances is well understood when the frequency of the disturbance is known, practically viable techniques to handle unknown frequencies have only recently emerged. A natural approach to reject a sinusoidal disturbance with unknown frequency is to construct a frequency estimator and use the estimated frequency in a disturbance cancellation scheme for known frequency. This concept is called an *indirect approach* in [3] [11], in analogy to the indirect methods of adaptive control. In contrast, direct methods attempt to design a stable adaptive controller for the rejection of the disturbance in a single and integrated algorithm. The direct algorithm of [3] is an extension of the concept of *phase-locked loop* (PLL) that has been called a *magnitude phase-locked loop* (MPLL). The MPLL algorithm was expanded to manage cases where the disturbance contained several harmonic components [1] and cases with multivariable plants [10]. A discrete-time MPLL was presented in [2], and an averaging analysis was given in [5], where the algorithm was also extended to handle the case of multiple uncorrelated sinusoidal components. The algorithm of this paper is based on the discrete-time MPLL concept of [5], with a focus on the case where two frequencies are very close. Advantages of the MPLL disturbance compensator are its relative simplicity and the ability to design easily a system with pre-specified closed-loop dynamics. In pure disturbance rejection problems such as active noise control, the algorithm can also handle high-order plants with complicated dynamics and significant delay without requiring an estimate of the plant transfer function. The algorithm uses the frequency response of the plant, which can be directly measured through sinusoidal excitation in a training stage.

Recently, researchers have considered frequency estimation and disturbance rejection problems where the frequencies of two independent sinusoidal signals must be tracked, including cases where the two frequencies were very close. Note that frequency tracking and signal reconstruction can be viewed as special cases of the disturbance rejection problem where the plant transfer function is the unity operator. [9] describes a problem where a sensor must be developed to measure mass flow in an agricultural machine. The spectrum of the sensor data shows a peak at 13.2 Hz, corresponding to the mass flow, together with a parasitic signal at 11.6 Hz, corresponding to the resonance frequency of the sensor. In [13], the problem of pitch tracking for automatic music transcription is considered. When multiple notes are played together (polyphonic case), the algorithm must track more than one sinusoidal component. The paper reports data for notes at 262 Hz and 392 Hz, but closer spacing may be encountered and could be as little as 6 percent. In [12], a disturbance rejection problem was considered in a web transport application. Experiments on the testbed showed that the spectrum of the tension had large disturbance components at the frequencies of rotation of the winding and unwinding rolls and that these frequencies could become identical.

This paper considers the problem of rejecting disturbances having two sinusoidal components

with close, unknown frequencies, and using feedback control. A natural approach to such problem consists in using two adaptive schemes such as MPLL's combined in parallel [5]. However, a problem with this approach is that convergence may be slow when the frequencies get very close to each other. It is known, from communications theory, that a sinusoid that is amplitude-modulated by a sinusoid of lower frequency has a spectrum reflecting the presence of two sinusoids with close frequencies. This paper is based on the reverse property that a pair of sinusoids can be represented as a single sinusoid with time-varying magnitude and phase. The observation is used to develop an adaptive disturbance rejection scheme, and its advantages and limitations over two parallel MPLL's are investigated on an ANC testbed.

2 Representing Two Sinusoids as a Single Time-Varying Sinusoid

Consider a signal with two sinusoidal components

$$d(k) = m_1 \cos(\omega_1 k + \phi_1) + m_2 \cos(\omega_2 k + \phi_2) \tag{1}$$

where m_1, m_2 are the magnitudes of the two components, ω_1, ω_2 are their frequencies, and ϕ_1, ϕ_2 are their initial phases. Let

$$
\begin{aligned}
\alpha_f(k) &= \frac{(\omega_1 + \omega_2)k + \phi_1 + \phi_2}{2} \\
\alpha_s(k) &= \frac{(\omega_1 - \omega_2)k + \phi_1 - \phi_2}{2}
\end{aligned}
\tag{2}
$$

and define the associated frequencies

$$\omega_f = \frac{\omega_1 + \omega_2}{2}, \ \omega_s = \frac{\omega_1 - \omega_2}{2} \tag{3}$$

Note that, if ω_1 and ω_2 are close to each other, ω_s is much smaller than ω_f. Accordingly, we will call ω_f the *fast frequency* and ω_s the *slow frequency*. The fast frequency is the average of the two original frequencies.

To lighten the notation in the following presentation, we will drop the time index k from α_f and α_s. However, the reader should remember that they remain functions of time. The following fact forms the basis of the paper.

Fact: the signal in (1) can be represented as a time-varying sinusoid of the form

$$
\begin{aligned}
d(k) &= m_d(k) \cos(\alpha_d(k)) \\
\alpha_d(k) &= \alpha_f(k) + \phi(k)
\end{aligned}
\tag{4}
$$

3

where

$$m_d(k) = \sqrt{m_1^2 + m_2^2 + 2m_1 m_2 \cos(2\alpha_s)} \tag{5}$$

$$\phi(k) = \arctan\left((m_1 - m_2)\sin\alpha_s, (m_1 + m_2)\cos\alpha_s\right) \tag{6}$$

The parameters m_d and ϕ of (5), (6) will be called the *nominal parameters*. An alternative expression is

$$m_d(k) = \sqrt{m_1^2 + m_2^2 + 2m_1 m_2 \cos(2\alpha_s)}\,\mathrm{sign}(\cos\alpha_s) \tag{7}$$

$$\phi(k) = \arctan\left((m_1 - m_2)\sin\alpha_s, (m_1 + m_2)\cos\alpha_s\right)$$
$$- \frac{1 - \mathrm{sign}(\cos\alpha_s)}{2}\pi \tag{8}$$

The parameters m_d and ϕ of (7), (8) will be called the *alternative parameters*.

Proof: from the definitions of α_f, α_s, the signal in (1) can be written as

$$d(k) = m_1 \cos(\alpha_f + \alpha_s) + m_2 \cos(\alpha_f - \alpha_s) \tag{9}$$

Therefore

$$d(k) = (m_1 + m_2)\cos\alpha_s \cos\alpha_f$$
$$- (m_1 - m_2)\sin\alpha_s \sin\alpha_f \tag{10}$$

Eq. (4) is obtained if $m_d(k)$ and $\phi(k)$ are chosen such that

$$(m_1 + m_2)\cos\alpha_s = m_d(k)\cos(\phi(k))$$
$$(m_1 - m_2)\sin\alpha_s = m_d(k)\sin(\phi(k)) \tag{11}$$

Indeed, for $m_d(k)$ as defined in (5) and for $\phi(k)$ as defined in (6), (11) holds. Therefore, (5) and (6) are valid. The alternative expression with (7), (8) follows directly from this result. $\square$

The fact indicates that a signal composed of two sinusoids can be represented as a single sinusoid with time-varying parameters. The expression for m_d in (5) shows that it depends on time through $\cos(2\alpha_s)$, so that m_d is a periodic function with frequency $2\omega_s$. Thus, if the frequencies of the two components are sufficiently close, the magnitude m_d varies at a frequency that is lower than the primary (fast) frequency ω_f. The following examples will show that a similar property holds true for the phase ϕ in (6), where ϕ is a periodic function with frequency ω_s. Fig. 1 shows a case where $m_1 = 2$ and $m_2 = 1$. The figure shows both the magnitude and the phase of the time-varying sinusoid as a function of α_s. If the frequencies are $\omega_1 = 0.01 \times 2\pi$ rad/sample and $\omega_2 = 0.011 \times 2\pi$ rad/sample, the fast frequency is $\omega_f = 0.0105 \times 2\pi$ rad/sample (corresponding to a period of about 95 samples) and the slow frequency is $\omega_s = 0.0005 \times 2\pi$ rad/sample (corresponding to a period of
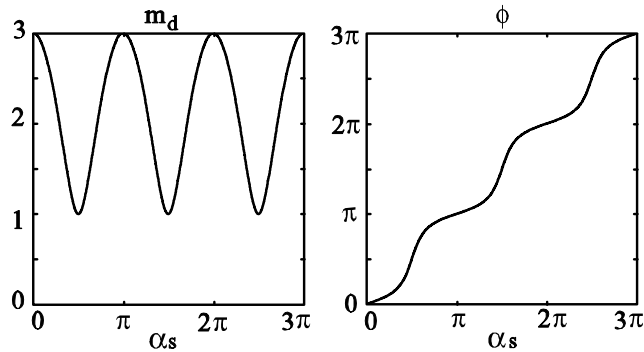
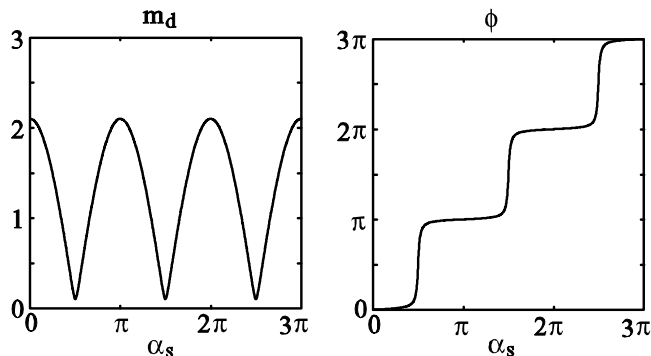Figure 1: Example with $m_1 = 2$ and $m_2 = 1$ and nominal parameters

Figure 2: Example with $m_1 = 1.1$ and $m_2 = 1$ and nominal parameters

2000 samples). The oscillations in the magnitude is about 10.5 times slower than the fast frequency ω_f, and the oscillations in the phase of the time-varying sinusoid is about 21 times slower than ω_f.

Unfortunately, while the magnitude and the phase parameters are periodic at the slow frequency, they may exhibit rapid changes, so they cannot always be assumed to be slowly-varying. At a time of rapid change, a system designed to track the parameters (such as a phase-locked loop) will have difficulties maintaining a small error. Rapid changes occur especially when $m_1 \simeq m_2$. Fig. 2 shows an example where $m_1 = 1.1$ and $m_2 = 1$ and the parameters of the time-varying sinusoid are specified by (5) and (6). The phase ϕ shows abrupt changes near $\alpha_s = \pi/2$, $3\pi/2$, and $5\pi/2$. In the extreme case where $m_1 = m_2$, the magnitude parameter becomes the absolute value of a sinusoid of frequency ω_s and the phase is a staircase signal that jumps by π when the magnitude is zero and is constant otherwise.

The limiting case where $m_1 = m_2$ is the motivation for the alternative parameters of (7) and (8). This formulation lets the magnitude parameter change sign, so that the phase parameter is equal to zero for all time. Both parameters are much smoother functions of time. When m_1 and m_2 are close but not equal, the alternative parameters are not as smooth as when $m_1 = m_2$, but nevertheless smoother than the nominal parameters. Fig. 3 shows the alternative parameters when $m_1 = 1.1$ and $m_2 = 1$. Note that m_d is discontinuous when $\alpha_s = \pi/2$, $3\pi/2$, and $5\pi/2$, but the jumps are small because $m_1 \simeq m_2$ (between $|m_1 - m_2| = 0.1$ and $-|m_1 - m_2| = -0.1$) and the
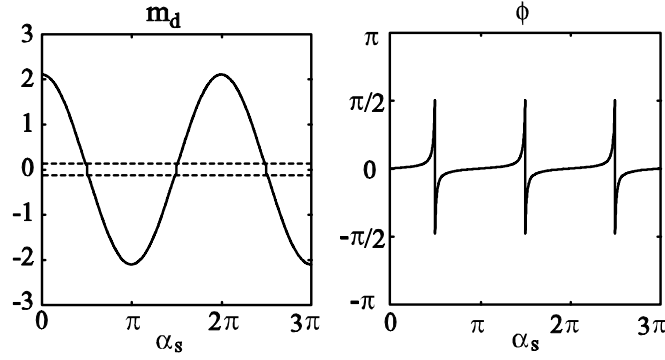
5

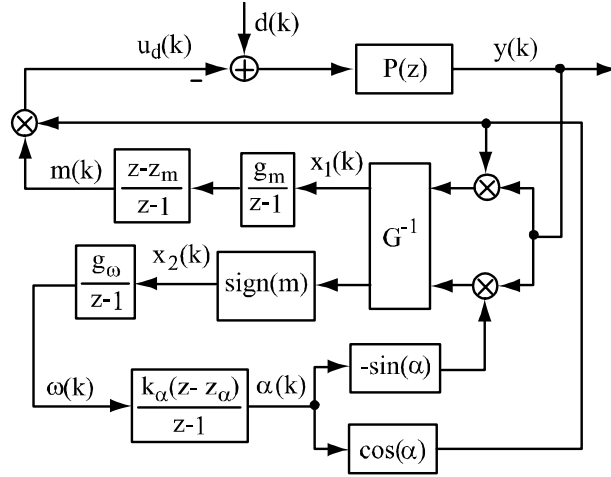Figure 3: Example with $m_1 = 1.1$ and $m_2 = 1$ and alternative parameters

Figure 4: Adaptive algorithm for the rejection of a sinusoidal disturbance with time-varying magnitude and phase

slope of the signal is smoother. The phase parameter exhibits rapid changes, but instead of a large jump, one finds a glitch of short duration. Further, the glitch occurs when the signal has small magnitude. Therefore, a system with limited bandwidth, such as a phase-locked loop, will "ride through" the glitch, with only a small impact on performance.

3 Two-As-One Disturbance Rejection Scheme

3.1 Adaptive Algorithm

We propose a new disturbance rejection algorithm based on the MPLL algorithm in [5] and the above representation of two sinusoids with close frequencies. In particular, we show how the algorithm can track a pair of sinusoidal disturbances as a single, time-varying sinusoid, and how the algorithm can be modified to improve performance when $m_1 \simeq m_2$. The structure of the proposed disturbance rejection system is shown in Fig. 4.

The plant is described by

$$y(z) = P(z)(d(z) - u_d(z)) \tag{12}$$

6

where $P(z)$ is the plant transfer function and is assumed stable, $d(z)$ is the z-transform of the input disturbance, and $u_d(z)$ is the z-transform of the disturbance compensation signal.

The disturbance d has the form of (1) with two sinusoidal components. Considering the alternative time-varying sinusoidal representation in (4), we can obtain the instantaneous frequency of d as

$$
\begin{aligned}
\omega_d(k) &= \alpha_d(k) - \alpha_d(k-1) \\
&= \omega_f + \phi(k) - \phi(k-1)
\end{aligned}
\tag{13}
$$

where ω_f is defined in (3) and ϕ in (6) or (8). The disturbance compensation signal has the form

$$
u_d(k) = m(k)\cos(\alpha(k))
\tag{14}
$$

where the signal m is the estimate of the magnitude m_d and the signal α is the estimate of the phase α_d. The signal ω is an estimate of ω_d, where ω_d is the instantaneous frequency of the disturbance (13). The goal of the algorithm is to obtain a good tracking performance despite the influence of the sinusoidal disturbance $d(k)$.

The equations of the algorithm in Fig. 4 are

$$
\begin{aligned}
\begin{bmatrix} x_1 \\ x_2 \end{bmatrix} &= \begin{bmatrix} 1 & 0 \\ 0 & \operatorname{sign}(m) \end{bmatrix} G^{-1} \begin{bmatrix} y\cos(\alpha) \\ -y\sin(\alpha) \end{bmatrix} \\
u_d &= m\cos(\alpha)
\end{aligned}
\tag{15}
$$

where G is a 2×2 matrix

$$
G = \frac{1}{2} \begin{bmatrix} P_R & -P_I \\ P_I & P_R \end{bmatrix}
\tag{16}
$$

and P_R and P_I are the real and imaginary parts of the plant frequency responses, evaluated at the nominal frequency ω_d, that is

$$
P_R = \operatorname{Re}[P(e^{j\omega_d})], \quad P_I = \operatorname{Im}[P(e^{j\omega_d})]
\tag{17}
$$

The remaining signals are given in the z-domain by

$$
\begin{aligned}
m(z) &= \frac{g_m(z - z_m)}{(z-1)^2} x_1(z) \\
\omega(z) &= \frac{g_\omega}{z-1} x_2(z) \\
\alpha(z) &= \frac{k_\alpha(z - z_\alpha)}{z-1} \omega(z)
\end{aligned}
\tag{18}
$$

The parameter k_α is chosen so that, for constant frequency ω, the phase α is the integral of the

frequency. Thus, $k_\alpha = 1/(1 - z_\alpha)$. The significant difference between this algorithm and the algorithm of [2], [5] is the presence of the $\text{sign}(m)$ term, which was inserted in the algorithm to allow the magnitude estimate to change sign. A pole was also added in the magnitude loop to improve the tracking of the time-varying magnitude parameter.

3.2   Approximate Analysis and Parameter Selection

We propose an analysis of the system based on a series of approximations inspired from the theory of phase-locked loops (it may be noted that the results can also be justified by the application of averaging theory for discrete-time systems [5]). The analysis assumes that m, m_d, ω and ω_d vary slowly. The adaptive parameters m and ω can be made to vary slowly by choosing small controller gains. The signal parameters m_d and ω_d vary slowly for large relative difference between m_1 and m_2, and for $m_1 = m_2$. In other cases, the approximation is valid, except around the discontinuity points. However, the jumps in m_d are relatively small and the short duration glitches in ϕ occur when the signal has small magnitude, so that the approximation is still useful. The next step is to assume that the response of the plant to d and u_d can be approximated by its sinusoidal steady-state response. Thus, the outputs can be computed based on the frequency response of the closed-loop system. Then, as is commonly in the theory of phase-locked loops, only the low-frequency components resulting from multiplication of two sinusoidal signals are kept in the equations. Finally, it is assumed that the instantaneous frequencies ω and ω_d are close enough that $P(e^{j\omega})$ can be replaced by $P(e^{j\omega_d})$.

Substituting (4) and (14) into (12), we obtain

$$
\begin{aligned}
y \simeq\ & P_R m_d \cos(\alpha_d) - P_I m_d \sin(\alpha_d) \\
& - P_R m \cos(\alpha) + P_I m \sin(\alpha)
\end{aligned}
\tag{19}
$$

After discarding of the high-frequency terms $\sin(2\alpha)$, $\cos(2\alpha)$, $\sin(\alpha + \alpha_d)$, and $\cos(\alpha + \alpha_d)$, we have

$$
\begin{aligned}
y \cos(\alpha) \simeq\ & \frac{1}{2} P_R m_d \cos(\alpha - \alpha_d) - \frac{1}{2} P_R m \\
& + \frac{1}{2} P_I m_d \sin(\alpha - \alpha_d)
\end{aligned}
$$

$$
\begin{aligned}
-y \sin(\alpha) \simeq\ & -\frac{1}{2} P_R m_d \sin(\alpha - \alpha_d) - \frac{1}{2} P_I m \\
& + \frac{1}{2} P_I m_d \cos(\alpha - \alpha_d)
\end{aligned}
\tag{20}
$$

The discarding is justified both by m_d and m varying sufficiently slowly and by the low-pass filtering
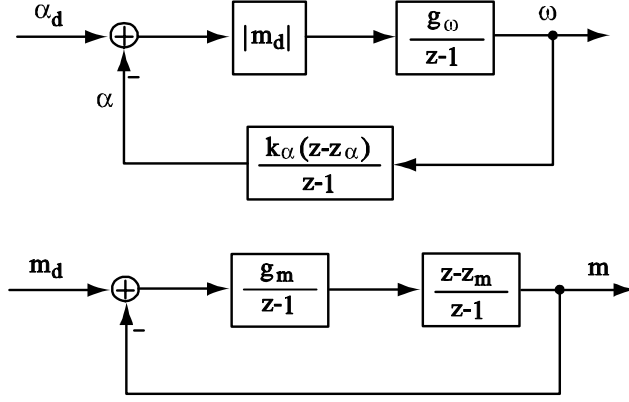
8

Figure 5: Linear approximation of the frequency loop (top) and magnitude loop (bottom)

occurring in the algorithm. A vector form of (20) is given by

$$
\begin{bmatrix} y\cos(\alpha) \\ -y\sin(\alpha) \end{bmatrix} \simeq G \begin{bmatrix} m_d\cos(\alpha - \alpha_d) - m \\ -m_d\sin(\alpha - \alpha_d) \end{bmatrix}
\tag{21}
$$

For small phase error, $\cos(\alpha - \alpha_d) \simeq 1$, $\sin(\alpha - \alpha_d) \simeq \alpha - \alpha_d$, and we obtain

$$
\begin{bmatrix} x_1 \\ x_2 \end{bmatrix} \simeq \begin{bmatrix} m_d - m \\ \mathrm{sign}(m)m_d(\alpha_d - \alpha) \end{bmatrix}
\tag{22}
$$

If the magnitude estimate tracks the magnitude signal well, $\mathrm{sign}(m) \times m_d \simeq |m_d|$ and

$$
\begin{bmatrix} x_1 \\ x_2 \end{bmatrix} \simeq \begin{bmatrix} m_d - m \\ |m_d|\,(\alpha_d - \alpha) \end{bmatrix}
\tag{23}
$$

Therefore, the dynamics of the system become decoupled, and the decoupled linear approximations of the frequency loop and of the magnitude loop are shown in Fig. 5. Note that G^{-1} in Fig. 4 cancels the phase shift induced by the closed-loop transfer function.

For the approximate frequency loop in Fig. 5 (top), the poles of the closed-loop system can be placed by appropriate choice of the controller parameters. If $z_{d,\omega}$ is some desired location in the z plane for the closed-loop poles of the approximate adaptive system (inside the unit circle), the following parameters will result in poles at that location

$$
g_\omega = \frac{(1 - z_{d,\omega})^2}{|m_d|}, \quad z_\alpha = \frac{1 + z_{d,\omega}}{2}
\tag{24}
$$

For the magnitude loop, if $z_{d,m}$ is the desired location of the poles, it is possible to place the two closed-loop poles at $z_{d,m}$ by letting

$$
g_m = 2(1 - z_{d,m}), \quad z_m = \frac{1 + z_{d,m}}{2}
\tag{25}
$$

9

To implement the algorithm, initial estimates of the magnitude and the frequency of the disturbance are needed to set the initial parameters g_ω and G^{-1}, which may then be updated as functions of m and ω, or be kept unchanged during the adaptation if the prior estimates are sufficiently precise. Since m_d is unknown and time-varying, a good solution consists in using an upper bound. The root locus of the frequency loop in Fig. 5 shows that the system is stable for all parameters m_d less than the upper bound. The response of the closed-loop system will simply be slower if the disturbance is lower than the upper bound.

It should be noted that the algorithm cannot achieve zero error in the presence of two sinusoids, even in the ideal case (where no measurement noise or plant uncertainty is added to the system). This is due to the fact that the disturbance parameters are not constant. However, the error will be small if the parameter variation is slow. The worst case occurs when m_1 and m_2 are close to each other but not equal. Simulations show that, even in this worst case, the algorithm can suppress most of the disturbance.

4   Active Noise Control Results

Experimental ANC Testbed: The algorithms for the rejection of two sinusoidal signals with close frequencies were implemented on an experimental ANC system developed at the University of Utah. The algorithm was coded in C language on a dSPACE DS1104 R&D controller board hosted in a PC. The sampling rate was 8 kHz. A single bookshelf speaker, located about 2 ft away from the error microphone, generated a signal constituting the noise source. The microphone signal was passed through an antialiasing filter and sent to the dSPACE system through an A/D converter. The controller output signal was passed through a D/A converter and a smoothing filter, then sent to a noise cancelling speaker placed approximately 1.5 ft away from the microphone. Both the speakers and the microphone were set in a horizontal plane at about 4 ft in height. For ANC, the plant consists in the dynamics of sound propagation from the noise cancelling speaker to the microphone together with the response of data converters and filters. The adaptive algorithms of this paper require knowledge of the frequency response of the plant $P(e^{j\omega})$, which was estimated rapidly and reliably in a training stage, using an *empirical transfer function estimate* (ETFE [8]) method [11]. After the training, the estimated model $\hat{P}(e^{j\omega})$ was fixed and used in the implementation of the algorithms. The real and imaginary parts of the frequency response were obtained at 91 frequencies, equally spaced between 50 Hz and 500 Hz, and the results were saved in a look-up table. In real-time application, the real and imaginary parts of the frequency response at the estimated frequency were obtained by linearly interpolating the look-up table. Fig. 6 shows the estimates of the plant frequency response. The phase response mostly consists of a linear phase associated with the delay due to sound propagation from the speaker to the microphone. The magnitude response shows a significant number of peaks and valleys due to acoustic resonances (such as reflections on the wall).
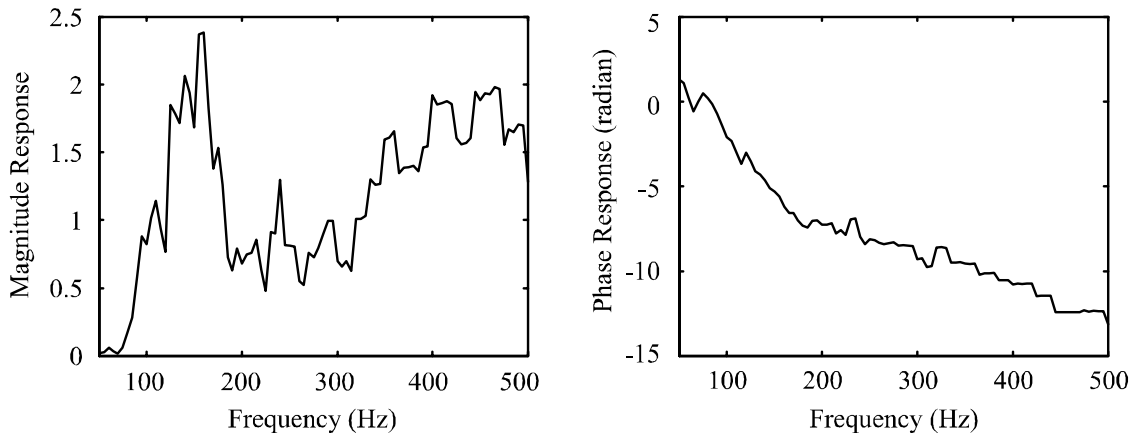
Figure 6: Frequency response of the plant: magnitude response(left), phase response (left).

ANC with Parallel Scheme: We first consider ANC experiments with a parallel scheme, with the goal of comparing the results to those obtained with the two-as-one algorithm proposed in this paper. The parallel scheme (please refer to Fig. 1 and Fig. 5 of [5]) consists of two replica of the disturbance controller in Fig. 4, but without the sign(m) term, and with only one pole in the magnitude loop. The algorithm was not engaged until 1 s (corresponding to 8000 steps), so that the amount of noise before compensation could be visualized.

In the first experiment, the disturbance had two sinusoidal components with frequencies at $0.02 \times 2\pi$ (160 Hz) and $0.03 \times 2\pi$ (240 Hz). The initial estimates were $\omega_{1,0} = 0.018 \times 2\pi$, $\omega_{2,0} = 0.032 \times 2\pi$, $m_{1,0} = m_{2,0} = 0$, and $\alpha_{1,0} = \alpha_{2,0} = 0$. The subscript index $1,0$ means the initial estimate for the first disturbance compensator, and $2,0$ is for the second one. The desired closed-loop poles were $z_{d,\omega} = 0.996$ and $z_{d,m} = 0.99$. The results can be seen in Fig. 7. They show that the algorithm, once engaged, reduced the noise significantly within 0.3 s. In contrast, Fig. 8 shows an experiment for a disturbance with much closer frequencies at $0.02 \times 2\pi$ and $0.021 \times 2\pi$. All the parameters were the same as the experiment in Fig. 7, except for $\omega_{2,0} = 0.023 \times 2\pi$. The two figures show that difficulties occur for closely-spaced frequencies, even though fast convergence rate had been achieved for widely-spaced frequencies. Fig. 9 shows that the problem with closely-spaced frequencies can be resolved by choosing smaller adaptation gains. The experiment is the same as Fig. 8 except that the frequency loop poles are located at 0.999 instead of 0.996. However, the convergence time is more than 3 seconds, instead of 0.3 seconds in Fig. 7. This is due to the smaller adaptation gains that were needed to ensure convergence in the closely-spaced case.

ANC with Two-as-One Scheme: The ANC experiment with the two-as-one scheme was performed for the disturbance in Fig. 9 with $\omega_0 = 0.0225 \times 2\pi$, $z_{d,\omega} = 0.996$ and the other parameters the same as the parallel scheme in Fig. 9. In this experiment, g_ω was set equal to $(1 - z_{d,\omega})^2/2$. The results are shown in Fig. 10, where one can see that the convergence time is less than 1 second, instead of about 3 seconds for the parallel scheme (see Fig. 9). Note that the frequency estimate converges to the average (fast) frequency $\omega_f = 0.0205 \times 2\pi$, as expected. The drawback is that there is a little more residual error in the microphone than the parallel scheme, an error associated
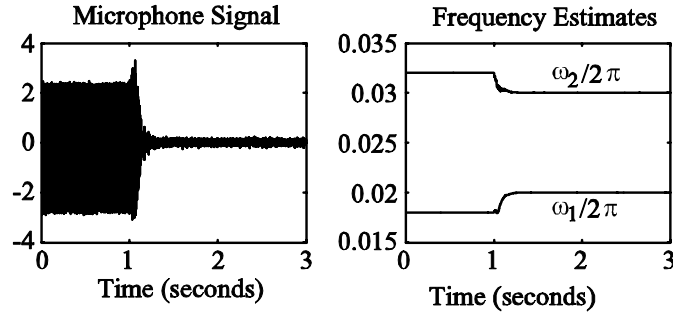
11

Figure 7: The microphone signal and two frequency estimates: widely separated frequencies and large adaptation gains case
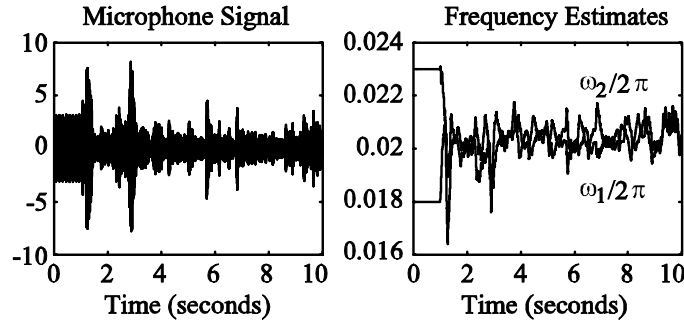

Figure 8: The microphone signal and two frequency estimates: closely spaced frequencies and large adaptation gain case

with the time variation of the signal parameters.

5 Conclusions

In this paper, an adaptive algorithm was presented for the rejection of disturbances having two sinusoidal components with close frequencies. The algorithm, called two-as-one scheme, rejected the disturbance as a single sinusoid with time-varying magnitude and phase. Theory was provided for the representation of the two components as a single one and the limitations of such a representation were discussed. A design method for the choice of the parameters of the disturbance rejection
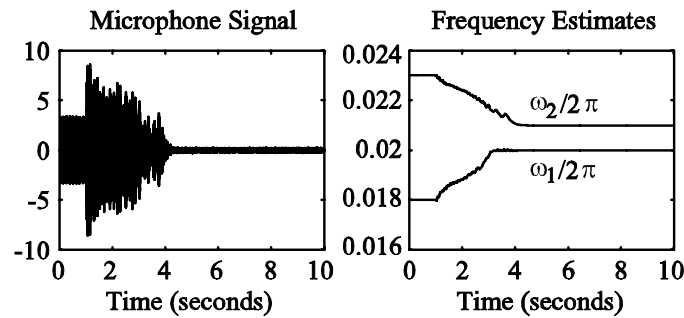

Figure 9: The microphone signal and two frequency estimates: closely spaced frequencies and small adaptation gains case
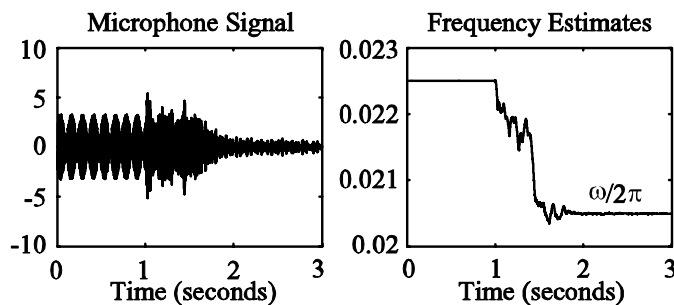
Figure 10: The microphone signal and frequency estimate for closely spaced frequencies: two-as-one scheme

algorithm was suggested, based on various approximations of the original system. The poles of an approximate, linear time-invariant closed-loop could be specified to match some desired values. Experimental results in active noise control showed that the two-as-one scheme had some advantages in terms of convergence, and that the $sign(m)$ term improved performance significantly in the cases that motivated its use. The two-as-one representation may also prove useful in other applications. It was found that, in some cases where well-known frequency estimation methods failed to discriminate between two close frequencies, one of the estimates that was obtained was the average frequency used in the two-as-one representation.

REFERENCES

[1] M. Bodson, J. S. Jensen, & S. C. Douglas, "Active noise control for periodic disturbances," *IEEE Trans. on Control System Technology*, vol. 9, no. 1, pp. 200–205, 2001.

[2] M. Bodson, "Performance of an adaptive algorithm of sinusoidal disturbance rejection in high noise," *Automatica,* vol. 37, no. 7, pp. 1133–1140, 2001.

[3] M. Bodson & S. C. Douglas, "Adaptive algorithms for the rejection of sinusoidal disturbances with unknown frequency," *Automatica,* vol. 33, no. 12, pp. 2213–2221, 1997.

[4] S. J. Elliott, I. M. Stothers, & P. A. Nelson, "A multiple error LMS algorithm and its application to the active control of sound and vibration," *IEEE Trans. on Acoustics, Speech, and Signal Processing,* vol. 35, no. 10, pp. 1423–1434, 1987.

[5] X. Guo & M. Bodson, "Analysis and implementation of an adaptive algorithm for the rejection of multiple sinusoidal disturbances," *IEEE Trans. on Control System Technology,* vol. 17, no. 1, pp. 40–50, 2009.

[6] S. Kim & Y. Park, "Active control of multi-tonal noise with reference generator based on on-line frequency estimation," *Journal of Sound and Vibration,* pp. 647–666, 1999.

[7] S. M. Kuo & D. R. Morgan, *Active noise control systems: algorithms and DSP implementations*, Wiley: New York, NY, 1996.

[8] L. Ljung & T. Glad, *Modeling of Dynamic Systems*, Englewood Cliffs: Prentice-Hall, 1993.

[9] K. Maertens, J. Schoukens, K. Deprez, & J. D. De Baerdemaeker, "Development of a smart mass flow sensor based on adaptive notch filtering and frequency domain identification," *Proc. of the American Control Conference*, pp. 4359–4363, 2002.

[10] B. Wu & M. Bodosn, "Direct adaptive cancellation of periodic disturbances for multivariable plants," *IEEE Trans. on Speech and Audio Processing,* vol. 11, no. 6, pp. 538–548, 2003.

[11] B. Wu & M. Bodson, "Multi-channel active noise control for periodic sources—indirect approach," *Automatica,* vol. 40, no. 2, pp. 203–212, 2004.

[12] Y. Xu, M. de Mathelin, & D. Knittel, "Adaptive rejection of quasi-periodic tension disturbances in the unwinding of a non-circular roll," *Proc. of the American Control Conference*, pp. 4009–4014, 2002.

[13] Z. Zhao & L. L. Brown, "Musical pitch tracking using internal model control based frequency cancellation," *Proc. of IEEE Conf. Decision and Cont.*, pp. 5544–5548, 2003.